International Journal of Power and Energy Systems, Vol. 42, No. 10, 2022
An Open Access Paper

REDUCED SWITCHING LOSSES IN THE INDIRECT MATRIX CONVERTER USING SINGLE RAMP CARRIER-BASED PWM SCHEME

Payal Patel* and Mahmadasraf A. Mulla**

Abstract

This work presents the single carrier-based pulse width modulation (CPWM) scheme which uses the ramp carrier instead of conventionally used triangular carrier in the existing single CPWM schemes. The use of ramp carrier reduces the switching losses of the indirect matrix converter by reducing the switching frequency of the load side converter (LSC) stage switches. It is shown that the existing single CPWM scheme utilizing the triangular carrier leads to the double switching frequency operation of the LSC stage switches in comparison with that obtained by the ramp carrier. The simulation and experimental results are presented to prove the effectiveness of the presented CPWM scheme of providing the required input and output performances. The simulation is performed in PSIM software, and the control devices TMS320F28335 DSP and Spartan-6 FPGA are used to develop the control algorithm in the hardware prototype. The switching losses of the presented CPWM scheme are compared with those in the CPWM scheme utilizing the single triangular carrier. The thermal module of PSIM software is utilized to find the switching losses in both methods.

Key Words

Carrier, FPGA (field programmable logic array), matrix converter, modulation scheme, pulse width modulation, THD (total harmonic distortion), voltage transfer ratio

1. Introduction

Matrix converter (MC) is an "all silicon" device which enables direct ac-to-ac conversion without any intermediate energy storing element. The important features of the MC are sinusoidal supply and load side waveforms, bidirectional power flow and adjustable input power factor [1]. The requirements of 18 bidirectional switches, complex modulation strategies, complex commutation and protection of the switching devices are the several disadvantages associated with the MC. The ac-to-ac conversion process of the MC is accomplished through either matrix of nine bidirectional switches or back to back connection of bidirectional rectifier and inverter stages. The former is known as the direct matrix converter and latter is known as the indirect matrix converter (IMC) topologies.

The space vector modulation (SVM) strategy is the most widely used and explored method for the MC due to its efficient performance in both balance and unbalance supply conditions [2, 3]. Several advantages associated with SVM method are the freedom of choosing the switching vectors and attainment of the maximum voltage transfer ratio (VTR) of 0.866 in the linear modulation range of operation without adding the third harmonics. However, the sector-based duty cycle calculations and lookup table-based determination of switching pulses make this modulation scheme very complex in the implementation.

In literature, several carrier-based pulse width modulation (CPWM) schemes have been investigated for the IMC to overcome the complexities of SVM scheme [4]–[10]. In [4], a CPWM method consisting of simple switching commutation and smooth sextant transitions is described for the MC topologies. The simple CPWM strategy is presented in [5] for the IMC, which reduces the complexity of modulation as compared to SVM technique. The CPWM method for increasing the VTR of the IMC beyond 0.866 is discussed in [6]. The carrier-based discontinuous PWM strategies for reducing the switching losses of the IMC are discussed in [7, 8]. However, the requirement of the carrier with the variable slopes for the modulation of the load side converter (LSC) stage of the IMC increases the complexity of realizing the above schemes. Additionally, in most of these modulation schemes, while the well-established CPWM schemes of the conventional inverter are employed for the LSC stage of the IMC, the source side converter (SSC) modulation get accomplished through the sector-based calculations. The CPWM method with the

* Department of Electrical Engineering, S. V. M. Institute of Technology, Bharuch, Gujarat 392001, India; e-mail: pppatel1980@gmail.com
** Department of Electrical Engineering, Sardar Vallabhbhai National Institute of Technology, Surat, Gujarat 395007, India; e-mail: mamulla@ieee.org
Corresponding author: Mahmadasraf A. Mulla
Recommended by Dr. Dwarkadas Pralhaddas Kothari
(DOI: 10.2316/J.2022.203-0413)

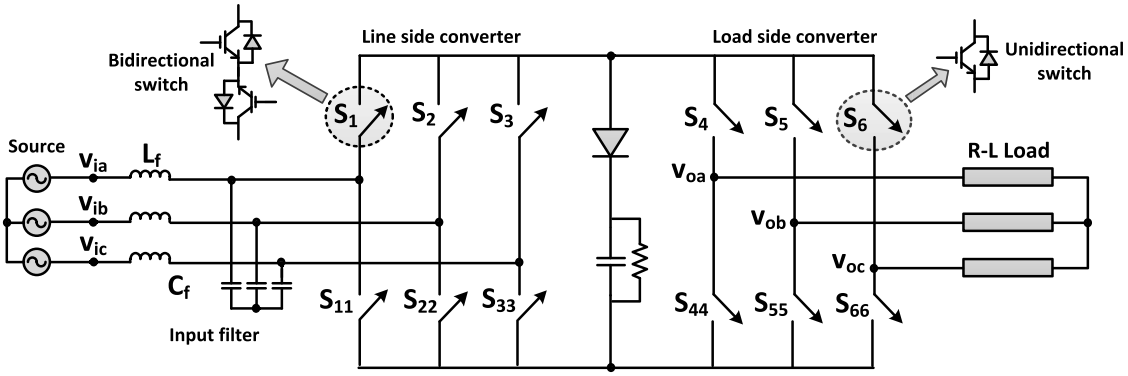

Figure 1. Indirect matrix converter topology.

single triangular carrier is proposed in [9] to reduce the implementation complexity of using variable slope carrier for the LSC stage. The duty cycles calculated in SVM technique are utilized to derive the modulation equations for the CPWM method presented in [9]. A simple single CPWM method is presented in [10] for the IMC which does not require the duty cycles calculated by SVM method to derive the modulation signals of the two converter stages. Both these single CPWM schemes presented in [9] and [10] are developed based on the symmetrical triangular carrier.

In this work, the CPWM method based on single ramp carrier is presented to control the IMC. The modulation principles used in the presented CPWM method are similar to those presented in [10]. The CPWM method in [10] uses the single triangular carrier to modulate the two stages of the IMC. It is shown in this work that the use of ramp carrier causes the switching devices of both stages of the IMC to modulate with the half switching frequency than that of the triangular carrier. However, the reduced switching frequency does not affect the SSC stage switching losses due to the zero current switching (ZCS) operation. But, the LSC stage switching losses are reduced when switching frequency is reduced due to the use of ramp carrier. The advantages of the presented CPWM scheme are the reduced switching losses of the LSC stage and the reduced complexity of implementation due to the use of single carrier. However, the total harmonic distortion (THD) of the output currents is slightly affected when ramp carrier is used instead of triangular carrier but not up to the great extent. The simulation and experimental results are presented to prove the effectuality of the proposed CPWM method. The simulation is performed in the PSIM software. The experimental setup of the IMC uses the control devices DSP TMS320F28335 and FPGA Spartan-6. The switching losses of the LSC stage of the IMC for the presented scheme are compared to those occur in the CPWM scheme with the single triangular carrier. To determine the switching losses, the thermal module of the PSIM software is utilized to develop the simulation model of the IMC.

The article is organized in six sections. Section 2 describes the modulation of IMC using CPWM scheme presented in [10]. Section 3 describes the modulation of the IMC with new CPWM scheme. The simulation and experimental results are included in Sections 4 and 5, respectively. The presented work is concluded in Section 6.

2. CPWM Scheme with Single Triangular Carrier [10]

Figure 1 shows the three-to-three phase IMC topology. The CPWM scheme presented in [10] is developed based on the CPWM principles of conventional rectifier and inverter topologies. It uses a single symmetrical triangular carrier to modulate the SSC and LSC stages of IMC. Figure 2(a) shows the modulation of the IMC using the CPWM scheme presented in [10]. m_{ia}, m_{ib} and m_{ic} represent the modulation signals of the SSC stage. For the given sampling interval T_s, the modulation signals m_{ia}, m_{ib} and m_{ic} constitute the maximum, medium and minimum amplitudes represented as M_{imax}, M_{imid} and M_{imin}, respectively. In the modulation of SSC stage, the comparison of M_{imid} with the symmetrical triangular carrier produces the two switching instants t_1 and t_2 as shown in Fig. 2(a). These two switching instants produce the switching durations $\frac{t_x}{2}$ and $\frac{t_y}{2}$ for the switches S_{22} and S_{33} in both halves of the sampling period T_s as verified in Fig. 2(a).

To synchronize the modulations of the two IMC stages, the modulation signals of the LSC stage are required to be modified in this scheme. m_{oa}, m_{ob} and m_{oc} are the modulation signals of the LSC stage of the IMC. Each output modulation signal is converted into the two signals based on the switching durations t_x and t_y created by the modulation of the SSC stage. Two modulation signals m_{oa1} and m_{oa2} are calculated for m_{oa} as given in (1) and (2).

$$m_{oa1} = m_{oa} \cdot m_{imid} \tag{1}$$

$$m_{oa2} = 1 - ((1 - m_{imid}) \cdot m_{oa}) \tag{2}$$

$$S_4 = S_4' \cdot S_4'' + \overline{S}_4' \cdot \overline{S}_4'' \tag{3}$$

The comparison of m_{oa1} and m_{oa2} with the triangular carrier produces the four switching instants t_3, t_4, t_5 and t_6 on the LSC stage. The switching instants at t_3 and t_6 produce the switching pattern S_4', whereas switching instants at t_4 and t_5 produce the switching pattern S_4''. By performing the exclusive NOR operation, the switching pattern S_4 is obtained as given by (3). It is observed that

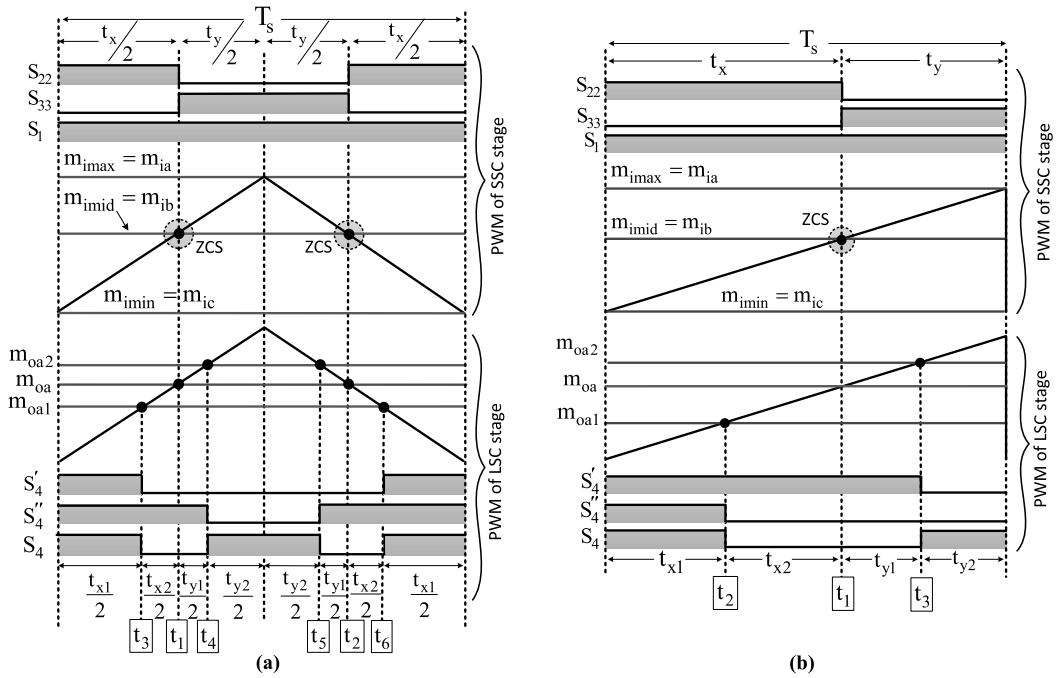

Figure 2. Modulation of two converter stages of IMC by CPWM scheme with: (a) Single triangular carrier and (b) single ramp carrier.

the gate signal S_4 consists of four switching transitions in one sampling period T_s. The synchronization of two stages of the IMC not only balances the input and output powers but also enables the SSC stage switching devices to work at zero currents which is known as ZCS. In ZCS operation, all the switching instants of the SSC stage switching devices aligned with the zero voltages states produced by the LSC stage. Resultantly, all the switching losses of the SSC stage are eliminated. However, the ZCS operation of the SSC stage is obtained as long as LSC stage is operating in the linear modulation range.

3. Proposed CPWM Scheme with Single Ramp Carrier

In this section, the modulation of the IMC using the proposed CPWM scheme is explained. The presented CPWM scheme employs the single ramp carrier to modulate the two stages of IMC. The modulation principles of SSC and LSC stages are same as in [10]. Therefore, all the advantages associated with the CPWM scheme in [10] are integrated in the presented scheme. The calculations of the modulation signals for the two stages of the IMC as well as the determination of gate pulses for the two stages remain same as in [10].

Figure 2(b) shows modulation of the two converter stages of IMC with the presented scheme. In the modulation of SSC stage, the comparison of M_{imid} with the carrier signal generates the switching instants of the SSC stage switching devices as explained in Section 2. It is observed that only one switching instant t_1 is created in sampling duration T_s on comparing M_{imid} with the ramp carrier. This switching instant creates the switching durations t_x and t_y for the switches S_{22} and S_{33}, respectively. Now, to modulate the LSC stage in synchronism with the SSC stage, two modulation signals for each of the output signal m_{oa}, m_{ob} and m_{oc} are required to be calculated. Figure 2(b) shows the comparison of m_{oa1} and m_{oa2} with the ramp carrier. The same equations, (1) and (2), are used to calculate the two modulation signals m_{oa1} and m_{oa2} for m_{oa}. The comparison of m_{oa1} and m_{oa2} with the ramp carrier generates the two switching instants t_2 and t_3 to produce the two switching patterns S'_4 and S''_4 as shown in Fig. 2(b). The switching patterns S'_4 and S''_4 are combined by (3) to produce the switching signal S_4 as shown. The ZCS operation of the SSC stage switching devices is obtained with the sawtooth carrier also similar to that with the triangular carrier.

It is observed from Fig. 2(b) that the total switching transitions in the gate signal S_4 are two in one sampling period T_s. This is half as compared to the switching transitions obtained by the CPWM scheme employed with the single triangular carrier as explained in Section 2. It clearly shows that the use of ramp carrier of the same frequency reduces the number of switching occurring on the LSC stage to the half as compared to that obtained with the triangular carrier. This leads to the reduced switching losses of the LSC stage and increased efficiency of the IMC.

4. Simulation Results

This section analyses the performance of the IMC using the new CPWM method based on the simulation results. The IMC model is developed in the PSIM environment. Various control and power circuit results are presented to verify the effectiveness of the presented CPWM scheme. The thermal module in PSIM is used to determine the

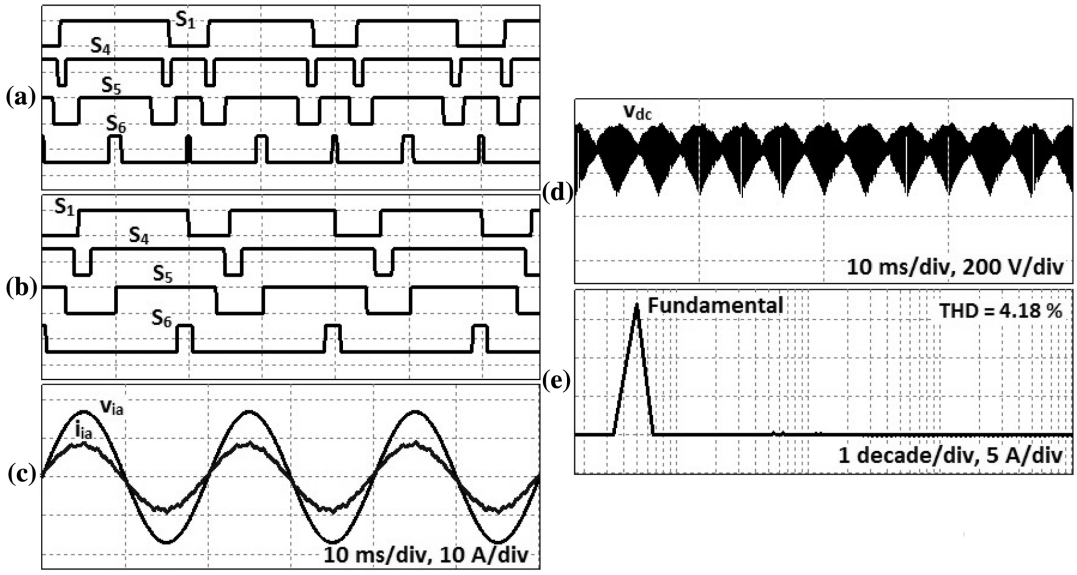

Figure 3. Simulation results: (a) Gate signals S_1, S_4, S_5 and S_6 obtained when modulations of two stages are carried out with single triangular carrier, (b) gate signals S_1, S_4, S_5 and S_6 obtained when modulations of two stages are carried out with new CPWM scheme with single ramp carrier, (c) supply voltage ($v_{\rm ia}$) and current ($i_{\rm ia}$), (d) dc-link voltage ($v_{\rm dc}$) and (e) harmonic spectrum of $i_{\rm ia}$.

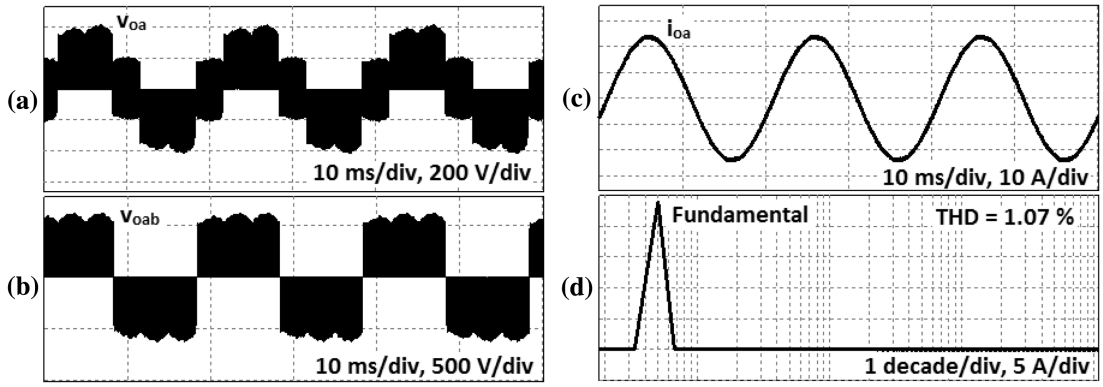

Figure 4. Simulation results of new CPWM scheme with single ramp carrier: (a) output voltage (v_{oa}); (b) output line voltage (v_{oab}); (c) load current (i_{oa}) and (d) harmonic spectrum of i_{oa}.

switching losses occur in the switching devices of the IMC. Based on this, the efficiencies of the IMC for the presented CPWM scheme are compared with those in the CPWM scheme employed with the single triangular carrier at the different carrier frequencies. The %THDs of the supply and load currents are also compared at the different carrier frequencies. The maximum ratings of the IGBT are 1200 V (V_{CES}), 25 A (I_C) and 150° (T_j). The various simulation parameters used in this work are: (a) supply voltage (V_s) = 245 V, (b) supply frequency (f_s) = 50 Hz, (c) load resistance (R_L) = 10 Ω, (d) load inductance (L_L) = 10 mH, (e) filter inductance (L_f) = 1 mH, (f) filter resistance (R_f) = 58 Ω, (g) filter capacitance (C_f) = 15 μF and (h) carrier frequency (f_c) = 10 kHz.

Figure 3(a) and (b) represents the gate signals S_1, S_4, S_5 and S_6 when triangular and ramp carriers are employed to modulate the two stages of IMC, respectively. It is shown that the number of switchings of the gate signals S_4, S_5 and S_6 is almost double in Fig. 3(a) than in Fig. 3(b). This indicates the effectiveness of using the ramp carrier for reducing the number of switchings of the LSC stage power devices. In both the cases, the ZCS operations of the SSC stage switching device are verified. Figure 3(c) shows the simulation waveforms of supply voltage (v_{ia}) and current (i_{ia}) with the presented CPWM scheme. The waveform of the supply current is near to sinusoidal nature. It is also observed from Fig. 3(c) that the input displacement angle between supply voltage and current is zero providing the unity power factor. Figure 3(d) represents the dc-link voltage (v_{dc}) which does not contain any zero voltage states as per the expectation. Figure 3(e) shows the harmonic spectrum of the supply current. It is shown that the lower order harmonics are almost absent in the supply current.

Figure 4(a) and (b) displays the load side phase and line voltages v_{oa} and v_{oab}, respectively. The waveforms

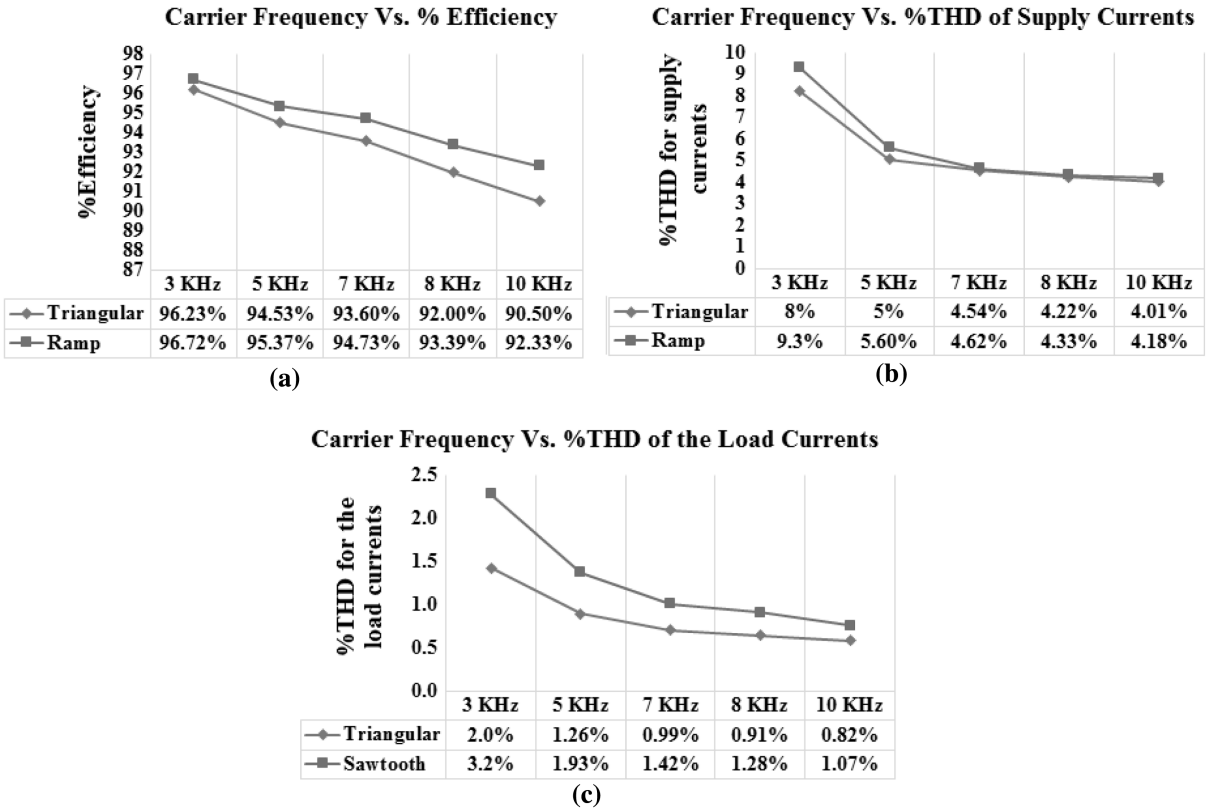

Figure 5. Comparison of new CPWM scheme and the CPWM scheme with single triangular carrier at different carrier frequencies based on: (a) % efficiency; (b) % THD of supply currents and (c) % THD of load currents.

obtained for the load quantities v_{oa} and v_{oab} are as per the expectation. Figure 4(c) shows the load current (i_{oa}) with the almost sinusoidal nature. The spectrum of the harmonics of the load current is shown in Fig. 4(d). The quality of the waveforms obtained proves that the use of ramp carrier does not affect the performance of the IMC.

Figure 5 compares the performances of the presented CPWM scheme and the CPWM scheme using the single triangular carrier at the different carrier frequencies. The comparisons are carried out at the carrier frequencies of 3, 5, 7, 8 and 10 KHz to analyse the performance of the IMC for % efficiency, % THD of the supply currents and % THD of the load currents. Figure 5(a) shows that the efficiency of the IMC is increased with the new CPWM scheme due to reduced switching losses as compared to that of the CPWM scheme using single triangular carrier. It is also observed that the % efficiencies are decreased in both CPWM schemes with the increased carrier frequency due to the increased switching losses. Figure 5(b) and (c) represents the comparison of modulation schemes based on the % THDs of the supply and load currents. It is observed that the supply and load current THDs in both the modulation schemes are improved with the increase in the carrier frequency. The % THDs of supply and load currents in new CPWM scheme are slightly more as compared to that in the CPWM scheme using single triangular carrier. These reduced values of THDs are due to the increased switching frequency in case of the CPWM scheme with the triangular carrier. However, in all the cases, the load current THDs are below 5% value.

The simulation study carried out in this section verifies the effectiveness of the new CPWM scheme. The expected performances of the IMC like the sinusoidal nature of input and output currents, dc voltage without zero voltage states, unity power factor, required output voltage waveforms and reduction in the switching losses prove the fruitfulness of the new CPWM scheme.

5. Experimental Results

The experimental results of the IMC modulated with the presented CPWM method are analysed in this section. The hardware platforms used to implement the CPWM method are 32-bit DSP (TMS320F28335) and FPGA (SPARTAN-6). The power IGBTs-FGA25N120ANTD by Fairchild semiconductor is utilized to realize source and load converters of the IMC. The various control and power circuit parameter values used in the hardware setup of the IMC are: (a) supply voltage (V_s) = 80 V, (b) supply frequency (f_s) = 50 Hz, (c) load resistance (R_L) = 10 Ω, (d) load inductance (L_L) = 10 mH, (e) filter inductance (L_f) = 2.7 mH, (f) filter resistance (R_f) = 68 Ω, (g) filter capacitance (C_f) = 15 μF and (h) carrier frequency (f_c) = 5 kHz.

Figure 6(a) shows the switching signals S_1, S_4, S_5 and S_6 which experimentally verifies the ZCS operation of the SSC stage switch S_1. These switching waveforms are similar to the simulation waveforms. The supply voltage and current waveforms obtained experimentally are shown in Fig. 6(b) which are similar in the nature to those obtained in the simulation. The dc voltage shown

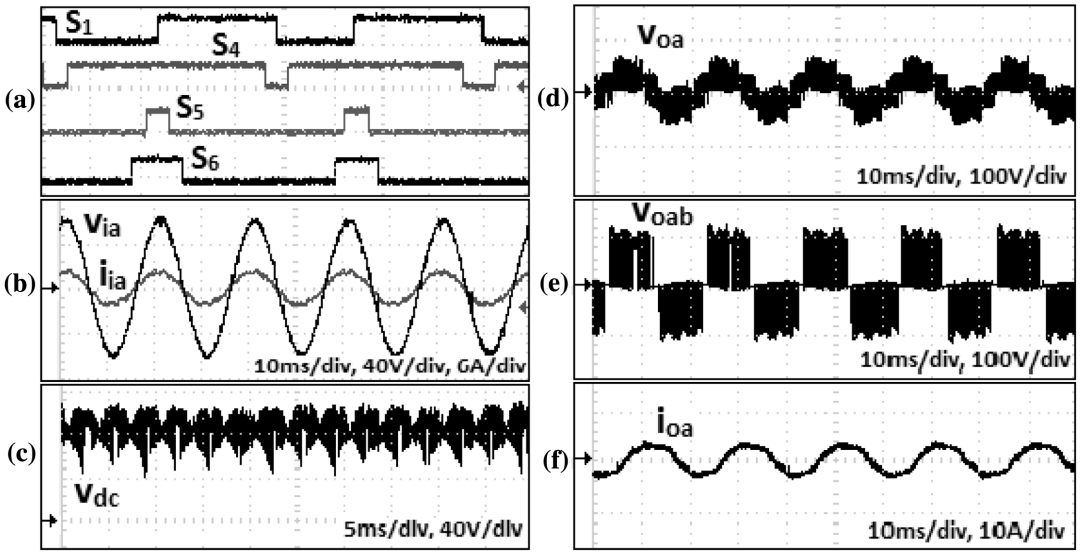

Figure 6. Experimental results of CPWM scheme with single ramp carrier: (a) gating signals S_1, S_4, S_5 and S_6 representing zero current switching of S_1; (b) supply voltage and current (v_{ia} and i_{ia}); (c) dc-link voltage (v_{dc}); (d) phase voltage on the load side (v_{oa}); (e) line voltage on the load side (v_{oab}) and (f) load current (i_{oa}).

in Fig. 6(c) is also matched with the dc voltage waveform obtained by the simulation. Figure 6(d), (e) and (f) represents the load side phase voltage, line voltage and load current, respectively, which are also similar to the simulation results.

In this section, it is verified that the presented CPWM scheme with the single ramp carrier is implemented as easily as CPWM scheme with the single triangular carrier. Also, the similarity of the input and output waveforms obtained by the simulation and the experiment validates the effectiveness of the presented CPWM scheme employed with the single ramp carrier.

6. Conclusion

In this work, a new CPWM scheme is presented for the IMC which uses the single ramp carrier for the modulation of the two stages of IMC. The presented CPWM scheme not only possesses the advantage of easy implementation due to the use of single carrier but also decreases the IMC switching losses. The presented work shows that the use of ramp carrier reduces the switching frequency of the LSC stage as compared to that obtained by the use of triangular carrier of the same frequency. This ultimately reduces the switching losses and thereby increases the efficiency of IMC. It is also shown by the simulation and hardware results that the presented CPWM method effectively provides the required supply and load side performances. By using thermal module of PSIM software, the ability of the presented CPWM scheme of providing the reduced switching losses in comparison with the CPWM scheme employed with the triangular carrier is presented.

References

[1] L. Empringham, J.W. Kolar, J. Rodriguez, P.W. Wheeler, and J.C. Clare, Technological issues and industrial application of matrix converters: A review, *IEEE Transactions on Industrial Electronics*, *60*(10), 2012, 4260–4271.

[2] S. Dabour and E. Rashad, Analysis and implementation of space-vector-modulated three-phase matrix converter, *IET Power Electronics*, *5*(8), 2012, 1374–1378.

[3] A.M. Bozorgi, M. Monfared, and H.R. Mashhadi, Two simple overmodulation algorithms for space vector modulated three-phase to three-phase matrix converter, *IET Power Electronics*, *7*(7), 2014, 1915–1924.

[4] P.C. Loh, R. Rong, F. Blaabjerg, and P. Wang, Digital carrier modulation and sampling issues of matrix converters, *IEEE Transactions on Power Electronics*, *24*(7), 2009, 1690–1700.

[5] B. Wang and G. Venkataramanan, A carrier based PWM algorithm for indirect matrix converters, in *2006 37th IEEE Power Electronics Specialists Conference*, 1–8.

[6] G.T. Chiang and J.-i. Itoh, Comparison of two over-modulation strategies in an indirect matrix converter, *IEEE Transactions on Industrial Electronics*, *60*(1), 2012, 43–53.

[7] Y. Bak and K.-B. Lee, Reducing switching losses in indirect matrix converter drives: Discontinuous PWM method, *Journal of Power Electronics*, *18*(5), 2018, 1325–1335.

[8] P. Patel and M.A. Mulla, Simple discontinuous PWM strategies to reduce the switching losses of an indirect matrix converter, *IET Power Electronics*, *13*(14), 2020, 2971–2982.

[9] D.-T. Nguyen, H.-H. Lee, and T.-W. Chun, A carrier-based pulse width modulation method for indirect matrix converters, *Journal of Power Electronics*, *12*(3), 2012, 448–457.

[10] P.P. Patel and M.A. Mulla, A single carrier based pulse width modulation technique for three-to-three phase indirect matrix converter, *IEEE Transactions on Power Electronics*, *35*(11), 2020, 11589–11601, doi: 10.1109/TPEL.2020.2988594.

Biographies

Payal Patel received the B. E. degree in electrical engineering from the S. V. M. Institute of Technology, Bharuch, India, in 2003, M. Tech. degree from the Sardar Vallabhbhai National Institute of Technology, Surat, India, in 2012 and Ph.D. degree from the Sardar Vallabhbhai National Institute of Technology, Surat, India, in 2021. Currently, she is working as an Assistant Professor in the Department of Electrical Engineering in S. V. M. Institute of Technology, Bharuch, India. Her research interests include electrical drives, power converters and power quality.

Mahmadasraf A. Mulla (IEEE S'97-M'11-SM'21) received the B. E. degree in electrical engineering from the Sardar Vallabhbhai National Institute of Technology, Surat, India, in 1995, M. E. degree from the Maharaja Sayajirao University of Baroda, Vadodara, India, in 1997 and Ph. D. degree from Sardar Vallabhbhai National Institute of Technology, Surat, India, in January 2015. He is currently an Associate Professor in the Department of Electrical Engineering, Sardar Vallabhbhai National Institute of Technology. His research interests include solar and wind energy conversion, electrical drives, power quality and active power filters.